2018

An Indicated Loss Analysis of a Light-Commercial Spool Compressor using High-Speed Pressure Measurements

Craig Bradshaw
Oklahoma State University, United States of America, craig.bradshaw@okstate.edu

Greg Kemp
greg.kemp@toradengineering.com

Joe Orosz
joe.orosz@toradengineering.com

Eckhard A. Groll
Purdue University - Main Campus, groll@purdue.edu

An Indicated Loss Analysis of a Light-Commercial Spool Compressor using High-Speed Pressure Measurements

Craig R. BRADSHAW[1*], Greg KEMP[2], Joe OROSZ[2], Eckhard A. GROLL[3]

[1]Oklahoma State University, Building and Environmental Thermal Systems Research Group, Stillwater, OK, USA, (405)744-5246
craig.bradshaw@okstate.edu

[2]Torad Engineering
Cumming, GA, USA, (678)366-3399
greg.kemp@toradengineering.com, joe.orosz@toradengineering.com

[3] Purdue University, Ray W. Herrick Laboratories, West Lafayette, IN, USA (765)494-2140,
groll@purdue.edu

* Corresponding Author

ABSTRACT

An analysis of the indicated and frictional losses is presented for a light-commercial prototype spool compressor. The spool compressor prototype was instrumented with four high-speed pressure sensors, three in the compression process and one in the discharge valve plenum. These sensors were triggered with a high-fidelity rotary encoder attached to the compressor motor shaft. This coupling of rotational position and pressure measurements allowed the development of an indicator (pressure v. volume) diagram for the compression process. Additionally, the added sensor in the discharge valve plenum allowed for a de-coupling of discharge valve losses and flow losses within the discharge plenum itself. The analysis shows that the suction and compression losses for this prototype compressor are relatively small compared with the discharge/valve losses. The total losses during the discharge process are generated by pressure drop and backflow through the discharge valve ports as well as when gas flows from the discharge plenum to out of the compressor body. The compressor was tested at three shaft speeds (900, 1300, 1620 rpm) at a condensing and evaporating temperatures ranging from 100 – 120 °F (37.8 – 48.9 °C) and 25 -60 °F (-3.8 – 15.6 °C), respectively at a fixed suction superheat of 30 °R (16.7 K). It was found that the total losses during the discharge process were the dominant indicated losses in the compressor and the discharge plenum losses accounted for between 32 and 66% of the total losses during the discharge process. The results suggest a 4-5% improvement in isentropic efficiency is possible by modifying the discharge plenum as well as improving the valve system.

1. INTRODUCTION

The rotating spool compressor is a novel rotary compressor mechanism most similar to the sliding vane compressor. Primary differences are described by Kemp *et al.* (2008) who first introduced the compressor applied to air-conditioning and refrigeration. Since its introduction the spool compressor has undergone a large development effort including several prototype generations to represent air-conditioning applications from residential split-systems to commercial chiller products. Each prototype platform has presented additional insight into the unique attributes of this compressor and the best application of the device. This was accomplished by leveraging each prototype platform to further explore the spool compressor attributes by studying specific phenomenon/sub-systems during development. The results of these studies are integrated in to the following prototype platform generation and continue to build the pool of knowledge for the spool compressor.

Orosz *et al.* (2012) presented the results of the 5th generation prototype spool compressor, a R410A device of roughly 3 tons of displacement, and compared its performance attributes such as efficiency trends with operating conditions against legacy compressor technologies. The study showed that the spool compressor had attributes that suggested it could potentially be an attractive option for part-load operation as a result of the lack of internal volume ratio. However, this generation spool compressor was unable to present a competitive efficiency and further study was required to understand the mechanisms for this.

Bradshaw and Groll (2013) then developed a comprehensive model of the spool compressor that provided a first-principles framework to begin to evaluate the spool compressor attributes in greater detail. As a result of early attempts of model validation it became clear that the dynamic sealing elements intrinsic to the spool compressor are of critical importance for model accuracy. Bradshaw (2013) then presented a sub-model for the comprehensive spool model specific to the tip sealing element and similar sub-models were developed for the spool seal (Bradshaw *et al., 2016)*. To better calibrate the model framework, it was necessary to generate an even deeper understanding of the individual processes occurring within the mechanism.

Bradshaw *et al.* (2016) presents a loss analysis based on dynamic pressure measurements within the 5th generation spool compressor prototype. The dynamic pressure measurements (when aligned with shaft angle) provide an analysis mechanism which enables evaluation of the indicated (flow) losses of a mechanism. By separating losses by the individual processes it is possible to deduce and/or narrow the potential loss mechanisms within the compressor. The loss analysis suggested that there were two key areas that required effort to increase the efficiency of the 5th generation spool compressor, the spool seals and the discharge valves. The analysis pointed to spool seals which were not adequately balanced and resulted in excessive leakage (indicated loss) and/or excessive friction depending on operating condition. Additionally, the discharge valves were identified in this study as one of the largest indicated losses. As a result, further development and optimization the valve system was performed with some of the most recent modeling presented in Wood *et al.* (2016).

In combination with the comprehensive model this analysis provides an important calibration mechanism which was used in the development of the 6th generation compressor. Orosz *et al.* (2014) presented the results from the 6th generation compressor, a R410A, roughly 5 tons of displacement, device. This generation prototype had competitive efficiencies with current market products with the same unique attributes presented previously. This result is suggestive of the fruitful gains possible with a rigorous study of the various sub-processes and sub-systems within a compressor, particularly a new technology.

The 7th and latest generation of prototype spool compressor presented initial performance data in Orosz *et al.* (2016) and shown in Figure 1. This R134a, 40 ton displacement, prototype was also designed using the aforementioned modeling tool. It was therefore expected to have measured efficiencies that were closer to optimum than the 5th generation despite this being the first R134a prototype, which was confirmed in Orosz *et al.* (2016). Despite the initial efficiency measurements it was clear that there may still be opportunity for improvement. To explore this, an indicated loss analysis will be performed on the 7th generation spool compressor prototype. This study will present the experimental methodology, data analysis techniques, and indicated loss analysis results and suggest changes to the 7th generation prototype to maximize its efficiency.

2. EXPERIMENTAL METHODOLOGY

The following section will describe the installation and setup of the experiment to collect an indicated loss analysis on the 7th generation spool compressor. This includes the sensor selection, placement, and calibration as well as an uncertainty analysis and the final test matrix of operating conditions which data was collected.

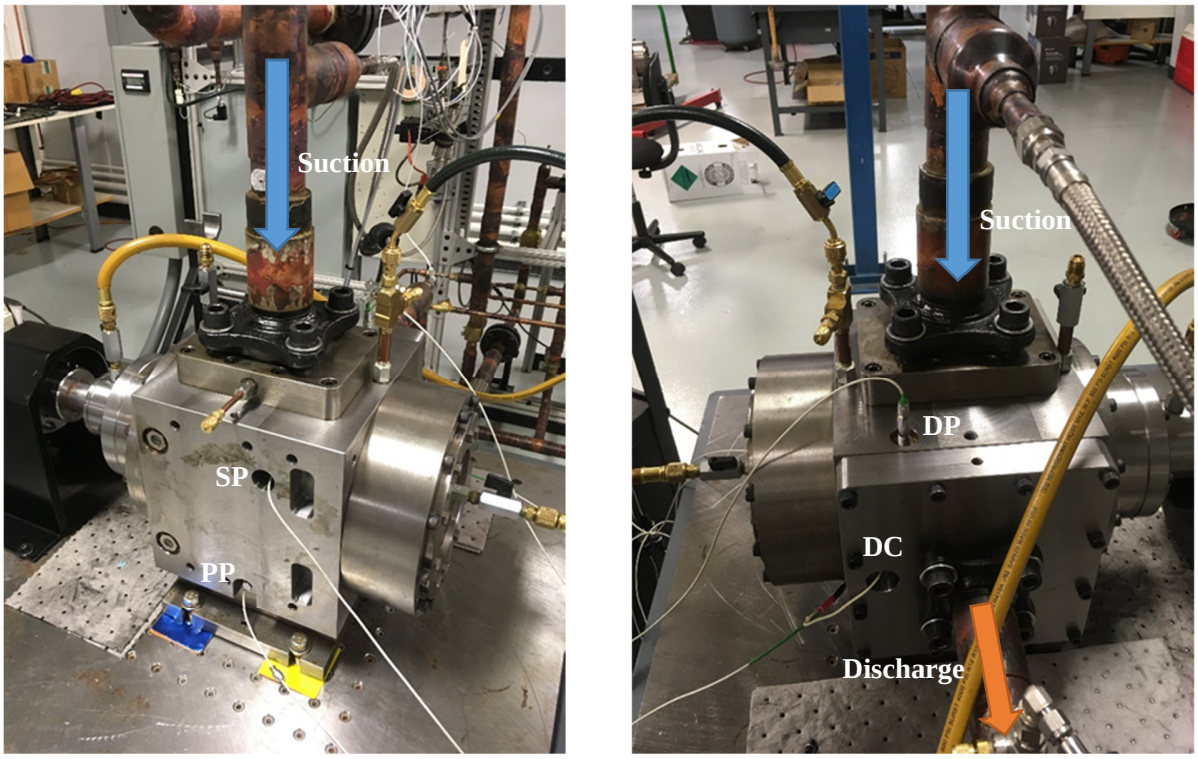

Figure 1: 7th generation, R134a, spool compressor prototype with high-speed pressure sensors installed showing suction (SP) and compression chamber (PP) sensor (left) and discharge (DP) and discharge cover (DC) sensor (right).

2.1 Sensor selection, location, calibration and procedure

A prototype spool compressor is fitted with three Endevco 8530B-500 high-speed pressure sensors at locations which will allow a majority of the process pressures to be measured at all rotor angles, called SP, PP, and DP, respectively. Additionally, and additional sensor is placed in the discharge plenum downstream of the discharge valve assemblies but upstream of the system plumbing connection, called DC. Figure 1 shows the physical locations of these sensors relative to the suction and discharge of the compressor. The left-hand figure highlights the sensors reading primarily the suction, SP, (top) and compression, PP, (bottom) processes while the right-hand figure shows the sensor reading the discharge process, DP, (top) as well as the sensor reading the discharge cover, DC, (bottom). The angular locations of the three sensors in the process are shown in Figure 2 which is a schematic of the compressor cylinder with vertical and the compressor Top-Dead-Center (TDC) identified. The only regions which cannot be measured are near the TDC area of the compression process on both the suction and discharge side of the compressor. Since the volume in this region is small it is assumed that any losses or phenomenon that is unable to be measured is also small.

The sensitivity of the piezoresistive transducers is susceptible to biasing and sensitivity shifts as a result of electrical installation (*i.e.* cable length and conductor quality) and mechanical installation. To mitigate this influence each of the four sensors was installed with 15 in-lbf of torque to mitigate sensor-to-sensor shifts due to mechanical installation. Each sensor was also calibrated in-place using dry nitrogen and a pressure reference measured using a Druck calibration device with an accuracy of 0.125 psia. The calibration was additionally repeated at the end of the first tests to ensure no significant changes to the calibration occurred.

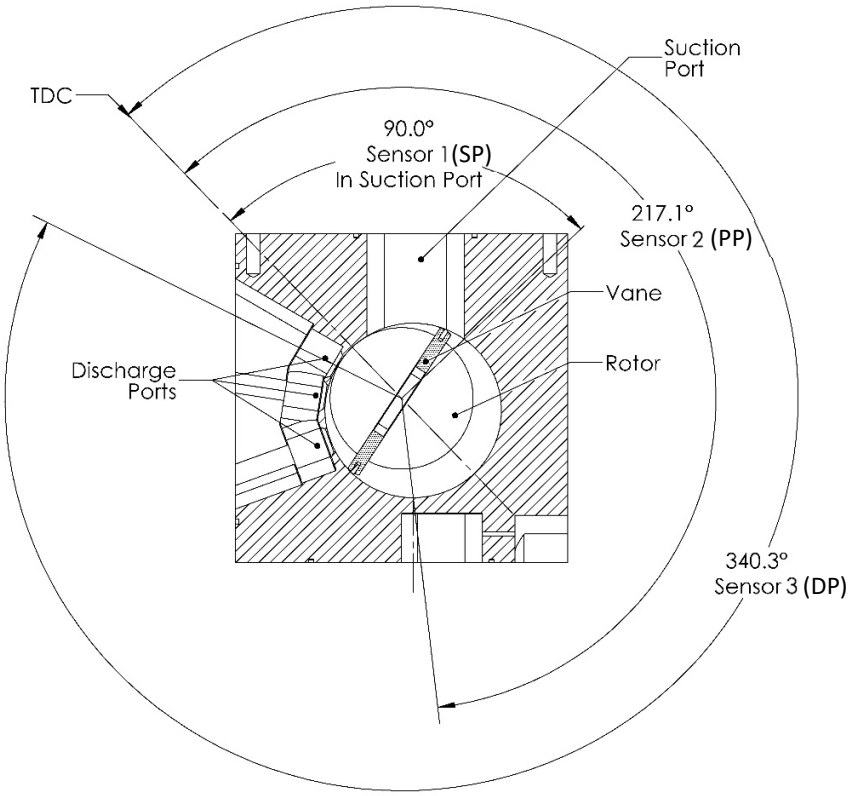

Figure 2: Angular location of in-pocket sensors relative to vertical and the compressor top-dead-center (TDC).

To measure shaft position, a rotary encoder was installed on the compressor motor shaft. The encoder is a model 702 quadrature encoder with index from the Encoder products company with 4096 steps per revolution. The encoder index was aligned with the compressor vertical and used to trigger data collection in the process described in the next section.

2.2. Experimental procedure and final test matrix

The compressor is first operated until it reaches steady state conditions at a prescribed operating condition using the hot-gas bypass load stand environment described in Orosz *et al.* (2016). The sensors are sampled at 70,000 samples per second for all conditions measured, triggered using the encoder index and sampled for 1 complete rotation of the shaft. This process was repeated 10 times per operating condition and these samples were collected into a single sample which reflects the behavior at the current condition.

The prototype compressor was operated using refrigerant R134a at three shaft speeds and saturated discharge temperatures (SDT) and various saturated suction temperatures (SST) at a fixed compressor inlet superheat of 30 °R for a total of 39 data points. The final test matrix collected for this study is presented in Table 1. The limited SST range for certain speeds and SDT are constrained by the limits of the test environment. The higher speed, lower SDT and higher SST conditions represent higher mass flow rates which were not possible to achieve with the test environment.

3. DATA REDUCTION AND ANALYSIS

This section will present the procedures used to reduce the collected data, estimate the uncertainty associated with the data and calculate the various indicated losses within the compressor.

Table 1: Final test matrix of 39 operating conditions (presented with various saturated suction and discharge temperatures, SST and SDT, respectively) with a fixed 30 °R superheat and shaft speeds high-speed measurements.

Speed	SST	Test #	SDT	Test #	SDT	Test #	SDT
rpm	°F	-	°F	-	°F	-	°F
900	25	1	100	9	110	17	120
	30	2	100	10	110	18	120
	35	3	100	11	110	19	120
	40	4	100	12	110	20	120
	45	5	100	13	110	21	120
	50	6	100	14	110	22	120
	55	7	100	15	110	23	120
	60	8	100	16	110	24	120
1300	25			25	110		
1620	25	26	100	28	110	33	120
	30	27	100	29	110	34	120
	35		100	30	110	35	120
	40		100	31	110	36	120
	45		100	32	110	37	120
	50					38	120
	55					39	120

3.1 Data reduction and uncertainty analysis

The uncertainty of the loss measurements is represented as a 95% confidence interval calculated using a two-tailed student's t-distribution. The values are calculated based an average of 10 samples per operating condition, collected as previously described, with a confidence interval calculated for the pressure at each crank angle. Figure 3 shows an example pressure vs. crank angle data for test number 12 which is an average of 10 data points that has the 95% confidence interval calculated at each instant in rotation. The figure shows that the uncertainty varies based on angular location but averages roughly 1 psia with outliers as high as 18 psia. Each condition was evaluated in a similar way with displayed similar confidence intervals. The global error associated with the pressure measurements is assumed to be the mean of confidence interval for the entire rotation. This global error estimate is used to estimate a propagated error associated with the losses presented, for Test #12 it is calculated to be 1.7 psia.

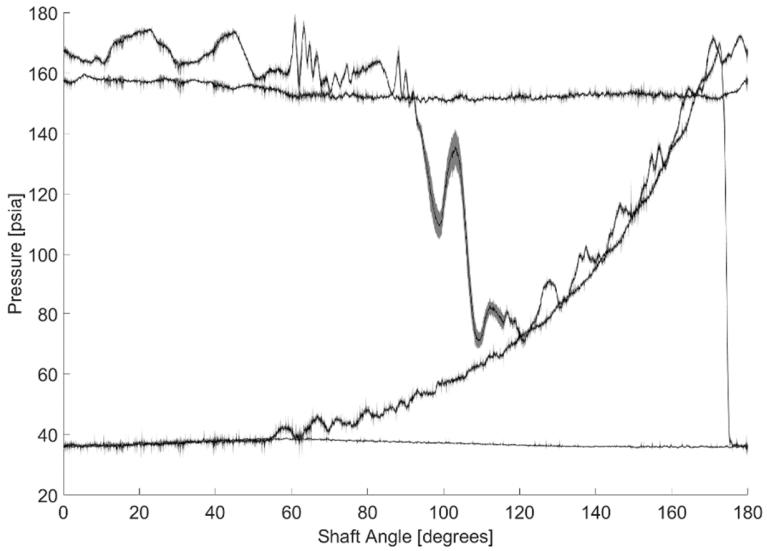

Figure 3: Example of final pressure curve with 95% confidence interval reported (gray shaded) for the average pressure recorded for Test #12.

3.2. Analysis of discharge losses

The discharge loss is a result of flow losses associated with the discharge port, valves, and flow from the discharge plenum to the system. Pressure drop associated with these three areas result in a chamber pressure that is higher than the discharge manifold (system) pressure to overcome these losses. This loss is illustrated in the left-side of Figure 4 and can be calculated using Equation 1 where the chamber pressure is equal to either the compression (PP) or discharge chamber (DP) during the discharge process depending on the vane location and operating condition. A majority of the test cases the entire discharge process is captured by the discharge sensor (DP), therefore the total discharge loss is calculated as,

$$L_{\text{discharge}} = \underbrace{-\int_{V_{\min}}^{V_{dis,start}} p_{DP}\,dV}_{w_{BW,dis}} - \underbrace{(p_{dis}(V_{dis,start} - V_{\min}))}_{w_{ideal}} \tag{1}$$

where the boundary work is integrated between the minimum compression volume and the volume corresponding with the cylinder pressure exceeding the discharge pressure measured in the system (p_{dis}). If a portion of the process is only captured by the compression chamber sensor (PP) the integration is piecewise computed using this sensor for the relevant volumes and this is added to the value from Equation 1.

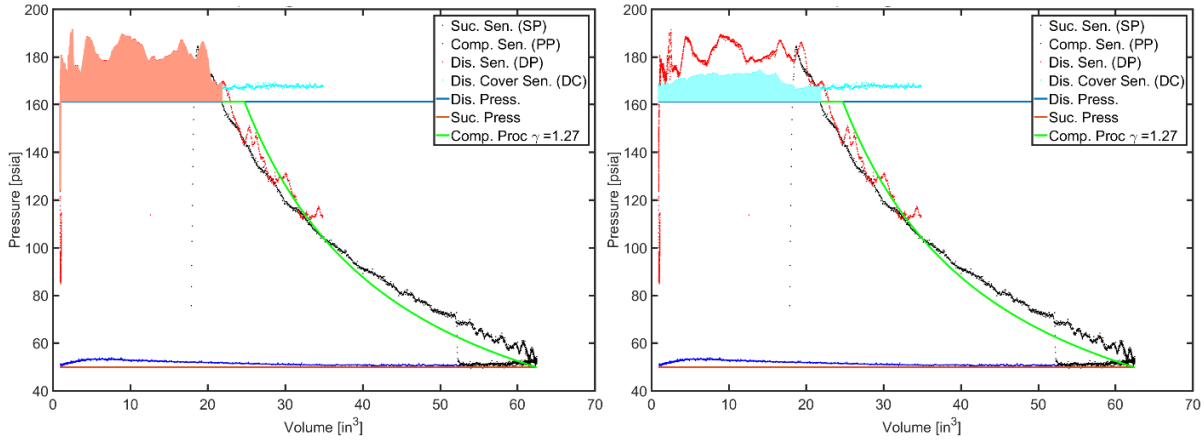

Figure 4: Indicator diagram of Test # 12 highlighting the areas representing the total discharge loss (left) and the discharge plenum loss (right)

To separately capture the losses associated with the losses associated with the fluid leaving the discharge plenumn (cover), the analysis of the discharge losses can also be calculated using the same technique but using pressure data collected from the discharge plenum (cover) transducer as shown in the right-side of Figure 4. This makes the assumption that the boundary work required to push fluid from the discharge plenum (cover) to the discharge pipe of the system requires the same change in volume as the discharge process itself. With this assumption, it is possible to directly extract the discharge losses associated with the valves by subtracting the total losses from the losses calculated using the pressure in the discharge plenum (cover),

$$L_{\text{dis,cover}} = \underbrace{-\int_{V_{\min}}^{V_{dis,start}} p_{DC}\,dV}_{w_{BW,\text{dis,cover}}} - \underbrace{(p_{dis}(V_{dis,start} - V_{\min}))}_{w_{ideal}}. \tag{2}$$

Finally, taking the difference between the cover losses and the total discharge losses the remainder is assumed to be dominated by the discharge valves/ports. Therefore, the valve losses are defined as,

$$L_{\text{valves}} = L_{\text{discharge}} - L_{\text{dis,cover}}. \tag{3}$$

3.3 Analysis of compression losses

The compression process losses are associated with pressure during the closed compression process and calculated relative to an isentropic compression process. An isentropic compressoion process is modeled using a polytropic compression process where the polytropic exponent is assumed to be the ratio of specific heats of the refrigerant calculated at the various suction conditions of the compressor.

Depending on operating condition, the discharge pressure (DP) sensor may capture a portion of the compression process that the compression process sensor (PP) does not. Therefore, a piecewise integration is typically necessary and the general loss definition is,

$$L_{\text{comp}} = \left[\underbrace{-\int_{V_{\max}}^{V_{trans.}} \left(p_{PP} - p_{ideal} \right) dV}_{\text{Under PP Curve}} \right] + \left[\underbrace{-\int_{V_{trans}}^{V_{dis,start}} \left(p_{DP} - p_{ideal} \right) dV}_{\text{Under DP Curve}} \right] \tag{4}$$

where p_{ideal} is the isentropic compression process, V_{trans} is the volume where the compression stops and discharge process begins, and $V_{\max}$ is the maximum volume of a single compression pocket.

3.4 Analysis of suction losses

Suction losses are associated with flow losses within the suction port as well as leakage that occurs during the suction process. These values are calculated using a similar procedure as the discharge process but requires the addition of the losses captured from two sensors, the suction (SP) and compression (PP) sensors which are both required to capture the entirety of the suction process. The loss is therefore given as,

$$L_{suction} = \underbrace{\left[\underbrace{-\int_{V_{\min}}^{V_{trans.}} p_{SP} dV}_{w_{BW,suc,1}} + \underbrace{\left(p_{suc} \left(V_{trans} - V_{\min} \right) \right)}_{w_{ideal,1}} \right]}_{\text{Under SP pressure curve}} + \underbrace{\left[\underbrace{-\int_{V_{trans}}^{V_{\max}} p_{PP} dV}_{w_{BW,suc,2}} + \underbrace{\left(p_{suc} \left(V_{\max} - V_{trans} \right) \right)}_{w_{ideal,2}} \right]}_{\text{Under PP pressure curve}} \tag{5}$$

4. RESULTS

Limited results are presented in the following section including a detailed breakdown of losses for the condition reflected by Test #12 and an analysis of the changes in discharge and cover losses with operating condition. The losses in this section are presented as percentage of relative total work measured from the compressor.

4.1 Losses at 40 °F SST, 110 °F SDT, and 900 rpm (Test #12)

Figure 5 shows a final indicator diagram of operating condition Test #12. Additionally, the bulk suction, discharge and calculated isentropic work pressure is also overlaid on top of the data as a basis of comparison. The indicator diagram is also presented in this figure with the loss areas calculated for each of the three main loss areas shaded to reflect the areas used in the analysis presented in the previous section. The results of the analysis for Test #12 are collected in Table 2 and broken down by percentage loss associated with each loss mechanism as a percentage of total compressor work.

Table 2: Collection of losses for Test #12 presented as a percent of total work.

Test #12 Results				
Discharge	**Valves**	**Cover**	**Suction**	**Compression**
%	**%**	**%**	**%**	**%**
11.70	6.20%	5.50	-3.30	1.48

This table shows that the total discharge loss is by far the largest loss at 11.7% with a large portion of that loss being associated with the cover losses (5.5%), leaving the remainder of 6.2% of valve losses. Both the cover and valve losses are significant but not one is as dominant as the discharge losses.

The negative suction loss reflects the suction pressure measured above the system pressure. This suggests that the measured suction process required less work than the ideal process. While this may be perceived as an advantage the caveat to this result is that work was required to compress the gas to a higher pressure than suction which then leaked back to the suction chamber to generate the higher pressure. Since that chain of events will result in more work than is saved it is advantageous to minimize the absolute value of this loss, in general. The measured phenomenon in Figure 5 appears to be a result of a small pressure rise at small volumes when change in volume being small. This could be associated with leakage at the top dead center clearance and/or the tip/side seals.

The compression loss is relatively small despite subjectively not matching the behavior presented in Figure 5. The actual process presents closer to isothermal than the isentropic process (*i.e.* polytropic exponent is less than specific heat ratio). Therefore, the specific work required is reduced and this results in a 'negative' loss for the portion of the process that approaches the start of the discharge process. This overcomes some of the additional work required to overcome the portion of the process just at the beginning of the compression process. It is hypothesized that the start of the compression process requires overcoming leakage losses and the negative portion of the compression process is associated with significant heat transfer from the compression pocket.

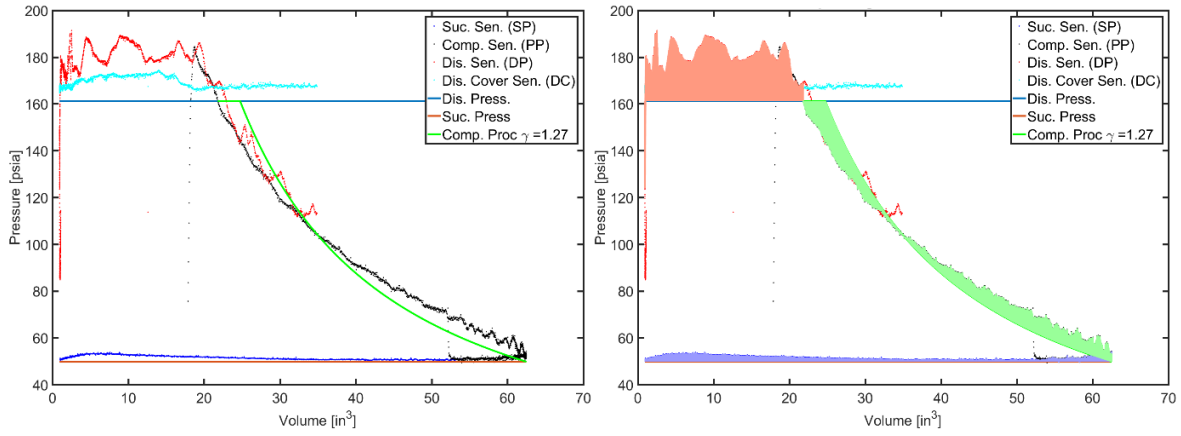

Figure 5: Indicator diagram of Test #12 with system suction and discharge pressures as well as the estimated isentropic compression process overlaid (left) and the loss areas shaded (right).

4.2 Discharge cover and valve losses

The discharge plenum (cover) and valve losses were the largest two components for Test #12 and this section will expanded on that analysis by presenting these losses with various operating conditions. Figure 6 presents both the discharge plenum (cover) and valve losses for both 900 and 1600 rpm compressor shaft speeds.

The plenum (cover) losses for both speeds and operating conditions show inconclusive trends. There does not appear to be a significant trend with either SDT or SST. Additionally, the differences between shaft speeds also seems

relatively minor. The analysis does show a persistent loss of between roughly 4-5% of efficiency are being lost a result of inadequate flow of gas from the discharge ports to the system.

The valve losses, also in Figure 6, show some significant trends. At both speeds, there is a slight dependency on SST with more valve losses at the highest SST's. However, more significantly is the dependency on SDT which presents in a more significant, and peculiar, way. At 900 rpm shaft speed the highest losses are at 110 °F SDT, followed by 100 °F and finally 120 °F with a maximum difference of nearly 4%. The 120 °F curve at 1600 rpm suggests a somewhat similar trend with SST but the trends in SDT do not appear as drastic nor trending in the same manner.

These losses could be associated with either the discharge valves or the valve port/port placement. The inconsistent loss behavior is suggestive of the trend being caused by a dynamic component with physics that are coupled to that of the system such as the response may not always be intuitive, such as is the case here. The dynamics associated with the discharge valves are a likely contributor to this response and should be further investigated to mitigate these trends.

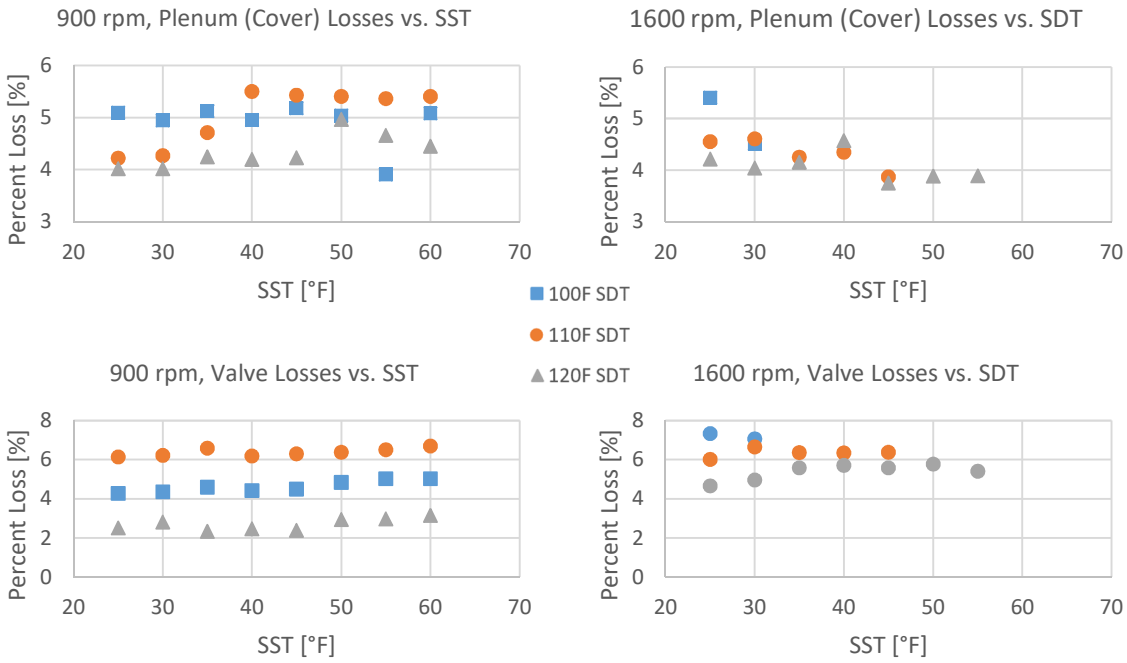

Figure 6: Indicated discharge cover (top) and valve losses (bottom) for various SST and SDT at both 900 rpm (left) and 1600 rpm (right).

5. CONCLUSION

This paper presents an indicated loss analysis for the 7th generation prototype spool compressor. The losses were collected using high-speed pressure measurements within the compressor with a synchronized encoder. The results suggest that the largest opportunity for improvement in this prototype is a re-design of the discharge plenum. This re-design has the potential to result in 4-5% improvement in the overall compressor efficiency.

Additionally, the valve improvements presented as another large potential improvement with losses ranging from 2-8% depending on speed and operating condition. The valve losses presented as somewhat independent of suction conditions but relatively sensitive to discharge conditions, particularly at slower speeds. The uniqueness of the discharge valve design (presented in Wood *et al.*,2016) in combination with these results indicates that more study of these types of valves is necessary to ensure the losses are mitigated across the entire operating range.

NOMENCLATURE

L	indicated loss	(Btu, kJ)
p	pressure	(psia, kPa)
V	volume	(in^3, m^3)
w	specific work	(Btu, kJ)

Subscript

BW	boundary work
comp	compression process
dis, cover	discharge cover portion of discharge
dis, start	start of discharge process
discharge	total discharge process
DC	discharge cover
DP	discharge pocket
ideal	ideal process
PP	process/compression pocket
suc, suction	suction process
SP	suction pocket
trans	transition between SP and PP sensors
valves	valve portion of discharge

REFERENCES

Bradshaw, C. Spool compressor tip seal design considerations. In 8th International Conference on Compressors and their Systems (2013), p. 341.

Bradshaw, C. R., and Groll, E. A. A comprehensive model of a novel rotating spool compressor. International Journal of Refrigeration 36, 7 (2013), 1974 – 1981. New Developments in Compressor Technology.

Bradshaw, C. R., Kemp, G., Orosz, J., and Groll, E. A. Development of a loss pareto for a rotating spool compressor using high-speed pressure measurements and friction analysis. Applied Thermal Engineering 99 (2016), 392–401.

Kemp, G. T., Garrett, N., and Groll, E. A. Novel rotary spool compressor design and preliminary prototype performance. In International Compressor Engineering Conference at Purdue University (2008), no. 1328.

Orosz, J., Bradshaw, C., Kemp, G., and Groll, E. Performance and operating characteristics of a novel rotating spool compressor. In International Compressor Engineering Conference (2012), no. 1257.

Orosz, J., Bradshaw, C., Kemp, G., and Groll, E. Updated performance and operating characteristics of a novel rotating spool compressor. In International Compressor Engineering Conference (2016), no. 1377.

Orosz, J., Kemp, G., Bradshaw, C. R., and Groll, E. A. An update on the performance and operating characteristics of a novel rotating spool compressor. In International Compressor Engineering Conference (2014), no. 1378.

Wood, N., Bradshaw, C.R., Kemp, G., Orosz, J., Groll, E.A. Dynamic modeling of a poppet valve for use in a rotating spool compress. In International Compressor Engineering Conference (2016), No. 1378.